

# Generation of octave-spanning spectra inside reverse-proton-exchanged periodically poled lithium niobate waveguides

Carsten Langrock,<sup>1,\*</sup> M. M. Fejer,<sup>1</sup> I. Hartl,<sup>2</sup> and Martin E. Fermann<sup>2</sup>

<sup>1</sup>Edward L. Ginzton Laboratory, Stanford University, Stanford, California 94305-4085, USA

<sup>2</sup>IMRA America, Inc., Ann Arbor, Michigan 48105, USA

\*Corresponding author: langrock@stanford.edu

Received May 24, 2007; accepted July 1, 2007;  
posted July 18, 2007 (Doc. ID 83395); published August 16, 2007

We demonstrate simultaneous octave-level spectral broadening and carrier-envelope-offset sensing of mode-locked Er- and Yb-doped femtosecond fiber lasers using constant-period and chirped reverse-proton-exchanged periodically poled lithium niobate waveguides. Chirped quasi-phase-matching gratings greatly improve spectral broadening of Yb-fiber lasers. © 2007 Optical Society of America  
OCIS codes: 120.3940, 190.4390.

In recent years, researchers have used highly nonlinear (HNL) and photonic crystal fibers to spectrally broaden the output of short-pulse mode-locked lasers for applications such as frequency comb generation [1], spectral fingerprinting, and coherence tomography [2]. One of the most important applications is carrier-envelope-offset (CEO) phase slip stabilization in order to generate phase-stable ultrashort pulses or, in the frequency domain, self-referenced frequency combs for frequency metrology applications [1].

CEO phase sensing is typically based on self-referencing schemes that require octave- or near-octave-spanning pulse spectra for their operation [3], directly available only from Ti:sapphire oscillators [4]. For nonoctave-spanning oscillators, including all-fiber-based lasers, self-referencing relies on the implementation of elements, usually separate, for spectrally broadening to the octave level and for the nonlinear frequency conversion steps required for phase sensing. Phase sensors not requiring harmonic generation have also been demonstrated but are usually more cumbersome to implement [5]. Typically, HNL and photonic crystal fibers have been used to generate octave-spanning spectra from mode-locked lasers, whereas bulk nonlinear crystals have been used for frequency conversion.

Recently, it has been shown by Fuji *et al.* that these two functionalities can be combined into a single optical element, namely bulk periodically poled lithium niobate (PPLN). It was used for spectral broadening of a broad-bandwidth Ti:sapphire oscillator to the full octave and simultaneous CEO sensing using a  $f-2f$  scheme with difference frequency generation of the high-frequency spectral part as the nonlinear step [6].

Guided-wave nonlinear optics significantly reduces the power requirement for CEO sensing because the efficiency of nonlinear interactions can be greatly increased by confining the input light to a small mode area over appreciable distances inside a waveguide. In conjunction with fiber lasers, we recently demonstrated that they allow for the construction of com-

pletely optically integrated frequency comb systems [7]. This work, however, still relied on HNL fibers for spectral broadening.

In this Letter, we show for the first time to our knowledge that spectral broadening of relatively narrow-bandwidth fiber laser sources centered at  $1.5\ \mu\text{m}$  and all required nonlinear interactions for CEO phase sensing using the  $2f-3f$  scheme can be combined in a single compact reverse-proton-exchanged (RPE) PPLN waveguide element. By optimizing device parameters, even octave-spanning spectra can be generated in these devices. In addition, we demonstrate significant spectral broadening of Yb-fiber lasers centered at  $1\ \mu\text{m}$  in RPE PPLN waveguides, where chirped poling periods greatly enhance the amount of spectral broadening. This technology potentially opens the way to ultracompact, phase-stable Yb-fiber lasers and Yb-fiber-laser-based frequency comb systems.

Schematics of our experimental setups are shown in Fig. 1. Light from an amplified mode-locked fiber laser was coupled into 33-mm-long RPE PPLN waveguide devices containing quasi-phase-matching (QPM) gratings with various lengths and periods. The amplified Er-fiber (Yb-fiber) laser produced 50 fs (150 fs) pulses with a center wavelength of 1580 nm (1043 nm) at an 86 MHz (90 MHz) repetition rate and output powers of up to 175 mW (1 W), corresponding to approximately 2 nJ (11 nJ) pulse energy and 37 kW (68 kW) peak power. The resulting output (30%–40% overall throughput, including 14% Fresnel

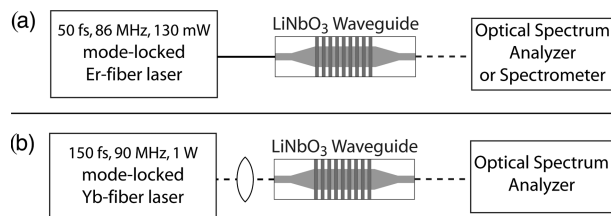


Fig. 1. Experimental setup showing the amplified mode-locked (a) Er-doped and (b) Yb-doped fiber laser and RPE PPLN waveguide device.

reflection at output facet and 0.2 dB/cm propagation loss) was then either coupled into a fiber to be measured using an optical spectrum analyzer (OSA) or free-space coupled into a scanning grating monochromator (SPEX Model 270M) with an InAs photodiode and lock-in detection. For CEO beat-note detection, the spectrum analyzer was replaced by a 10-nm-bandwidth interference filter and a Si-APD (Hamamatsu).

Figure 2(a) shows the visible and near-infrared (NIR) spectral components generated inside 12- $\mu\text{m}$ -wide and 2.3- $\mu\text{m}$ -deep RPE PPLN waveguides with 28- $\mu\text{m}$ -period QPM gratings of two different lengths [quasi-phase matched for second-harmonic generation (SHG) at a 2.4  $\mu\text{m}$  fundamental wavelength], pumped by the Er-fiber laser. We observe that the overall spectral content does not significantly change, while the strengths of the (higher-order) quasi-phase-matched components increase with grating length. The presence of a peak at 1.2  $\mu\text{m}$  even with the shorter (5.8 mm) grating indicates the presence of power at 2.4  $\mu\text{m}$ . The spectrum of the mode-locked fiber laser is superposed for reference (dashed curve). We can clearly see a spectral overlap between the second (medium gray area) and third harmonic (dark gray area) of the broadened laser

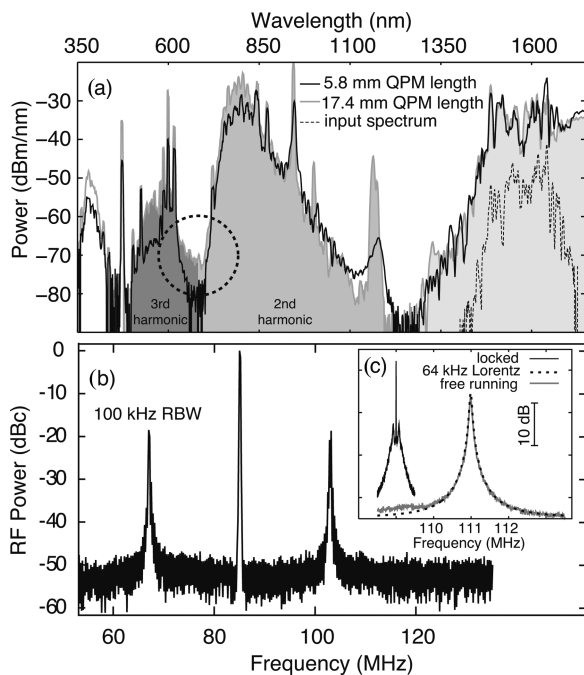


Fig. 2. (a) Visible and NIR spectral components created inside the waveguide by doubling (medium gray area), tripling (dark gray area), and quadrupling (white area) of the broadened (light gray area) input laser spectrum (dashed curve) for two different QPM grating lengths, 5.8 (black solid curve) and 17.4 mm (light gray solid curve). The distinctive spikes in the data correspond to (higher-order) QPM interactions. (b)  $f_{\text{rep}}$  and CEO-related beat signals detected in a 10-nm-wide spectral slice around 700 nm using a Si-APD. (c) Zoom into the CEO-related beat signals. The free-running beat signal can be fitted with a 64-kHz Lorentzian line shape. When phase locked to an RF synthesizer, the center of the beat note collapses to a resolution-bandwidth-limited coherent peak.

spectrum (light gray area). In this spectral overlap region around 700 nm, marked with a dashed circle, we could observe CEO-related beat signals via the  $2f-3f$  scheme on a RF spectrum analyzer with up to 30 dB signal-to-noise ratio [see Fig. 2(b)]. This beat signal could be stably phase locked to an RF synthesizer using the oscillator diode pump current for self-referencing of the frequency comb for several hours [see Fig. 2(c)]. Long-term locking was limited only by mechanical drifts of the alignment stages used for butt coupling to the waveguide, which can be eliminated by direct bonding of the fiber to the waveguide.

Using a scanning grating monochromator in combination with order filters, we measured the IR spectra out of the Er-fiber-laser-pumped RPE PPLN waveguide as a function of QPM grating period and length [8]. While we saw in Fig. 2 that the visible and NIR part of the spectra changes only slightly with increasing QPM grating length, it is apparent that the IR portion becomes significantly wider. The spectra shown in Fig. 3(a) exhibit more than an octave between 1420 and 2840 nm at the  $-30$  dB spectral power level with respect to the peak power level. The spectral components near the zero (SHG) group-velocity mismatch (GVM) wavelength around

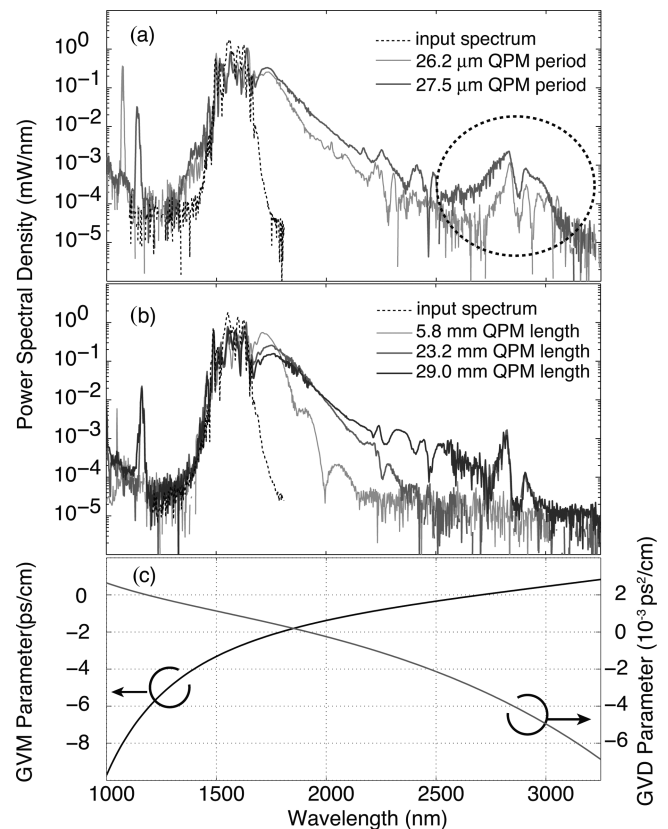


Fig. 3. Infrared spectra out of an Er-fiber-laser-pumped RPE PPLN waveguide as a function of (a) QPM grating period and (b) QPM grating length (28  $\mu\text{m}$  period) taken with a scanning grating monochromator; energy of pump pulses was 1.2 nJ. The dashed circle in (a) marks spectral components located near the zero SHG GVM wavelength. The spectrum of the mode-locked fiber laser is shown in black (dashed curve). (c) Plot of GVM for SHG, and GVD at fundamental wavelength, for bulk lithium niobate (extraordinary wave) from dispersion data of [9].

2750 nm have been marked with a dashed circle. A plot of the SHG GVM and group-velocity dispersion (GVD) parameters for the extraordinary wave in bulk lithium niobate [9] (approximately the same for weakly confined waveguides) is shown in Fig. 3(c), suggesting the difference-frequency-generation origin of the marked spectral components. Numerical simulations exploring the broadening mechanisms are currently underway.

Switching to the Yb-fiber laser as the pump source, we measured the spectra out of the RPE PPLN waveguide as a function of QPM grating period, power, and QPM grating chirp rate using an OSA (see Fig. 4). Here the observed spectral broadening was less pronounced than in the previous case. To obtain significant spectral broadening, chirped PPLN waveguides were used. The widest spectra were obtained for a poling period linearly chirped from 7 to 11  $\mu\text{m}$  over a 29-mm QPM-grating length. As shown in Fig. 4(c), spectral broadening exceeding 2/3 of an octave at the  $-40$  dB spectral power level with respect to the peak power level was obtained in the op-

timum case; the spectral region beyond 1700 nm was cut off by the limited range of the OSA. These RPE PPLN waveguides were deeper (2.3  $\mu\text{m}$ ) than the ones used for telecommunication applications (1.85  $\mu\text{m}$ ) and had a cutoff wavelength around 4  $\mu\text{m}$ . The pulse energy requirements for near-octave-spanning spectra in PPLN waveguides at Yb wavelengths were estimated to be around 6 nJ, similar to typical requirements for photonic crystal fibers. Numerical modeling should allow for establishing optimum chirp rates and QPM grating lengths to minimize these power requirements while maximizing the amount of spectral broadening. Actual CEO phase sensing will further require the implementation of additional constant-period frequency conversion sections.

We demonstrated octave-level spectral broadening of Er- and Yb-doped femtosecond fiber lasers inside RPE PPLN waveguides. Furthermore, we demonstrated that these devices can be integrally coupled to an Er-fiber laser system for simultaneous spectral broadening and CEO phase sensing. Using chirped PPLN devices, significant spectral broadening of a Yb-fiber laser to more than 2/3 of an octave was demonstrated. We believe chirped PPLN waveguides can play an important role in future compact phase-stable laser and frequency comb systems.

This research was sponsored by the Air Force Office of Scientific Research (AFOSR grant FA9550-05-1-0180), the Defense Advanced Research Projects Agency through the University of New Mexico Optoelectronic Materials Research Center (DARPA Prime MDA972-00-1-0024), and Crystal Technology, Inc.

## References

1. D. J. Jones, S. A. Diddams, J. K. Ranka, A. Stentz, R. S. Windeler, J. L. Hall, and S. T. Cundiff, *Science* **288**, 635 (2000).
2. I. Hartl, X. D. Li, C. Chudoba, R. K. Ghanta, T. H. Ko, J. G. Fujimoto, J. K. Ranka, and R. S. Windeler, *Opt. Lett.* **26**, 608 (2001).
3. J. Ye and S. T. Cundiff, eds., (Springer, 2005).
4. R. Ell, U. Morgner, F. X. Kärtner, J. G. Fujimoto, E. P. Ippen, V. Scheuer, G. Angelow, T. Tschudi, M. J. Lederer, A. Boiko, and B. Luther-Davies, *Opt. Lett.* **26**, 373 (2001).
5. P. A. Roos, X. Q. Li, R. P. Smith, J. A. Pipis, T. M. Fortier, and S. T. Cundiff, *Opt. Lett.* **30**, 735 (2005).
6. T. Fuji, J. Rauschenberger, A. Apolonski, V. S. Yakovlev, G. Tempea, T. Udem, C. Gohle, T. W. Hänsch, W. Lehnert, M. Scherer, and F. Krausz, *Opt. Lett.* **30**, 332 (2005).
7. I. Hartl, G. Imeshev, M. E. Fermann, C. Langrock, and M. M. Fejer, *Opt. Express* **17**, 6490 (2005).
8. C. Langrock, I. Hartl, M. E. Fermann, and M. M. Fejer, 2006 IEEE Lasers and Electro-Optics Society Annual Meeting (IEEE Lasers and Electro-Optics Society, 2006), paper PD1.4.
9. D. H. Jundt, *Opt. Lett.* **22**, 1553 (1997).

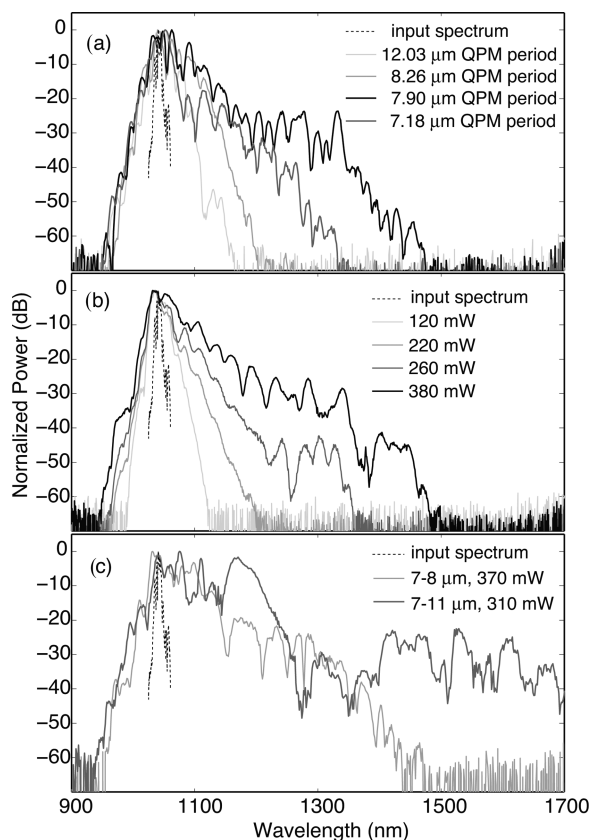


Fig. 4. NIR spectra out of a Yb-fiber-laser-pumped RPE PPLN waveguide as a function of (a) QPM period at fixed power (350 mW after the waveguide), (b) input power at fixed period (7.9  $\mu\text{m}$ ), and (c) QPM chirp rate. The input spectrum of the Yb-fiber laser is shown in black (dashed curve).